ICAS Paper No. 68-09

DETAILED EXPLORATION OF THE COMPRESSIBLE, VISCOUS FLOW OVER TWO-DIMENSIONAL AEROFOILS AT HIGH REYNOLDS NUMBERS

by

M. C. P. Firmin and T. A. Cook
Aerodynamics Department
Royal Aircraft Establishment
Farnborough, U.K.

The Sixth Congress of the International Council of the Aeronautical Sciences

DEUTSCHES MUSEUM, MÜNCHEN, GERMANY/SEPTEMBER 9-13, 1968

Preis: DM 2.00

DETAILED EXPLORATION OF THE COMPRESSIBLE, VISCOUS FLOW OVER TWO – DIMENSIONAL AEROFOILS AT HIGH REYNOLDS NUMBERS

M. C. P. Firmin and T. A. Cook
Royal Aircraft Establishment, Farnborough, Hampshire, England

Abstract

Wind-tunnel investigations into the flow over two-dimensional aerofoils are discussed with particular emphasis on the influence of viscous effects on aerodynamic characteristics. The experimental work was undertaken using large-chord-models spanning tunnels both with solid and slotted walls at the Royal Aircraft Establishment. The measurements were made with Reynolds numbers up to 15×10^6 and speeds up to high subsonic with models having a span-to-chord ratio of about 3.

Measurements of boundary layer and wake development are presented with more detailed measurements in the region of the trailing-edge of the wings. The results are compared with methods of estimation, and wind tunnel wall corrections are discussed.

Introduction

The design of aircraft for flight at high subsonic speeds has resulted in shapes that have a swept wing layout. In general, the sweep angles are such that the flow over the wings is sensibly similar to that over two-dimensional sections, and current trends would suggest that this situation will continue but with sections that more closely approach the boundaries imposed by viscosity and compressibility. As it is not yet possible to make exact calculations of the viscous compressible flow about aerofoils, prediction methods rely on sound experimental backing; yet as we explain in this paper, even experiments on two-dimensional sections are by no means as simple as the theoretical model might imply since they require particularly careful planning and meticulous attention to detail.

In the past, it has not been possible at speeds where compressibility was significant, to determine the influence of viscosity on the pressure distribution over an aerofoil as no general solution for potential-flow existed. Recently Sells[1] has obtained numerical solutions for the exact inviscid compressible flow over aerofoil sections at subcritical speeds. This is an important step forward and means that any difference between measured and theoretical pressure distributions, such as that shown in Figure 1 at high subsonic speeds, must now be limited to the viscous effects which we wish to investigate and any undesirable environmental effects due to the conditions under which measurements are made. These environmental problems include the constraining influence of the wind-tunnel walls and viscous effects, both of which may detract from the two-dimensionality of the tests. These problems have to be overcome before the influence of the viscous effects on two-dimensional aerofoils can be determined accurately. An example of some experimental results is given in Figure 1 and they have been corrected for the increased velocity over the aerofoil due to the presence of the wind-tunnel walls when the aerofoil is at zero lift (i.e. the blockage correction) but not for other wind-tunnel wall corrections, which would increase the difference in the quoted lift coefficients by about 0.03 assuming first order theoretical wall corrections apply. The inviscid flow calculations for this figure have involved an extrapolation from just below the critical speed which cannot be justified on purely theoretical grounds, but since the measurements themselves are wholly subcritical this is considered reasonable.

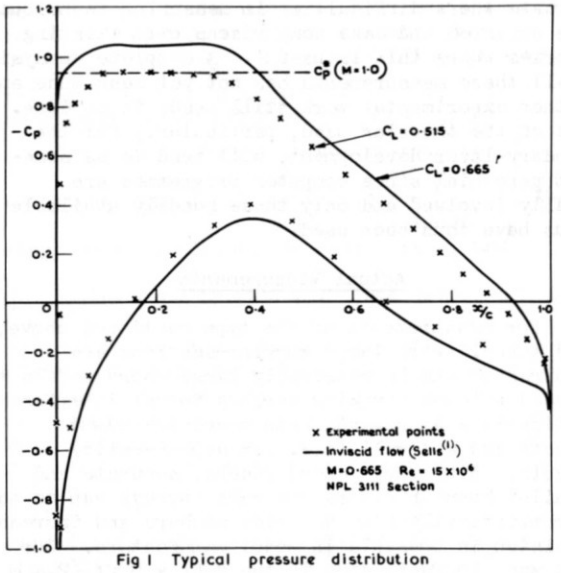

Fig 1 Typical pressure distribution

Viscous effects of course, occur due to flow in regions of high shear such as in the boundary layer and in the wake. At high Reynolds numbers, the flow in these viscous regions is usually turbulent and consequently not amenable to theoretical treatment unless simplifying assumptions are made. The viscous layers have thus to be determined experimentally. It should be possible however to treat these layers as normal boundary layers and wakes with constant static pressure normal to the surface, except near the trailing edge of an aerofoil where the flow curvature may be large. Küchemann[2] even suggests it is possible for the influence of vorticity in the curved flow near the trailing-edge to cause earlier separation than would otherwise be expected. Consequently, detailed measurements of the flow in such a region are particularly desirable.

When considering the overall forces on an aerofoil, the contribution to the lift from the frictional forces can usually be neglected and the lift determined from surface pressures alone, but for drag the frictional forces are important. The aerofoil drag is made up in two parts; the form drag, obtained from the surface pressures on the wing and due to the displacement effect of the boundary layer, and the frictional drag which has to be measured by some other means. Wake traverse methods, in which convenient assumptions are made about the flow, can be used to determine overall drag, but doubts still remain about the accuracy of such methods so direct measurements of the drag are also desirable.

There was, therefore, a need to design an experiment in which as much information as possible is obtained about the detailed flow characteristics.

The work must obviously be at high Reynolds numbers (so that boundary layer transition problems are reduced as much as possible) and at the high subsonic speeds relevant to present swept wing designs. Also it is essential that the conditions under which the wings are tested be known accurately, in particular the effects of wind tunnel wall interference, which are known to increase rapidly at the higher subsonic speeds, must be determined carefully.

In this paper we will give details of a selection of the measurements made so far at R.A.E., indicate where difficulties in measuring techniques have occurred and make comparisons with existing theories where this is useful. A complete analysis of all these measurements has not yet been made and further experimental work still needs to be done. Some of the theories used, particularly for the boundary-layer development, will tend to be somewhat parochial since computer programmes are usually involved and only those readily available to us have thus been used.

Actual Measurements

For measurements of the type mentioned above, wind tunnels with large working-sections are required to enable reasonably large chord models to be used without invoking serious tunnel interference difficulties as regards both chord-to-height effects and end-wall (i.e. low aspect-ratio) effects. With large chord models, accurate and detailed boundary-layer and wake surveys can be made at realistically-high Reynolds numbers and increased precision is possible in model manufacture. Our work was, in fact, done in the 8 ft × 8 ft (2.4 m × 2.4 m) closed-wall tunnel at Bedford and the 8 ft × 6 ft (2.4 m × 1.8 m) slotted-wall tunnel at Farnborough using models of up to 76 cm chord. Thus, both the model span-to-chord and tunnel height-to-chord ratios were 3 (or greater) while the trailing-edge boundary-layer thicknesses were typically 1 to 3 cm.

In the 8 ft × 8 ft (2.4 m × 2.4 m) tunnel, a wing was mounted as shown in Figure 2. Boundary layer and wake measurements were made using rear-mounted traversing probes. The wing was split into seven similar spanwise parts each individually mounted, so that it was possible to make overall force measurements on a central segment of the wing using a straingauge balance. The small gaps between the segments were sealed other than when overall force measurements were being made. In the 8 ft × 6 ft (2.4 m × 1.8 m) tunnel the wing was mounted vertically as shown in Figure 3. Boundary-layer and wake probes were mounted from within the thickness of wing and traversed by remotely controlled drives. Enlargements are shown of the probes protruding from the wing. Measurements in the wake further downstream than 10% of the chord behind the wing were made using rear-mounted traversing probes. This arrangement made sure that the influence of the probes and their supports on the flow over the wing was kept to an absolute minimum and that the location of the probes was known accurately even for measurements in the wake close to the trailing-edge of the wing. The wall slot arrangement was altered for this work, the open-area ratio of the walls parallel to a spanwise generator being varied by using additional plates behind the usual slots, and the slots in the walls normal to a spanwise generator were closed except for a region well downstream of the wing. Another wing was tested with the same section but having about half the chord so that tunnel interference effects could be investigated. The smaller wing did not have provision for making boundary layer measurements, however.

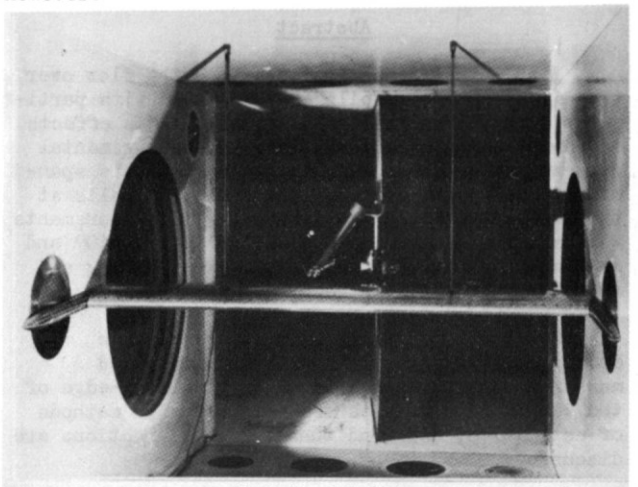

Fig.2: Aerofoil mounted in 8 ft x 8 ft (2,4 m x 2,4 m) wind tunnel

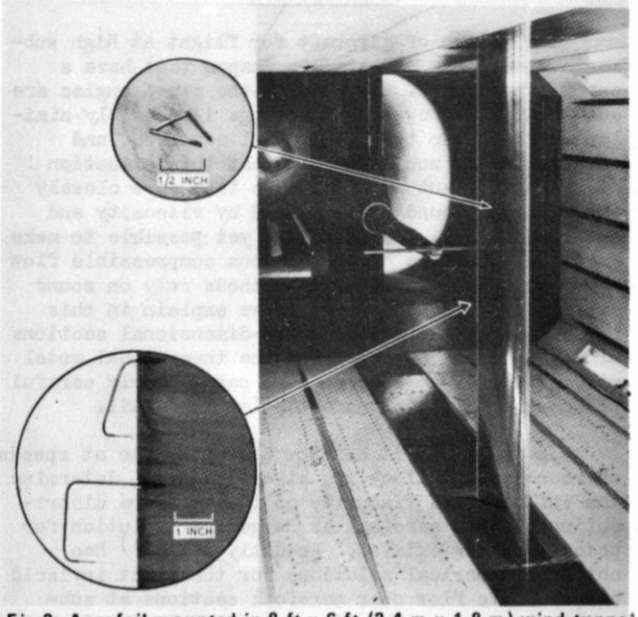

Fig.3: Aerofoil mounted in 8 ft x 6 ft (2,4 m x 1,8 m) wind tunnel showing remotely controlled boundary layer probes

In all the work comprehensive measurements of surface pressures were made while surface tube techniques were used for skin friction measurements.

On the models, boundary-layer transition problems have as far as possible been avoided by fixing transition with a sparse distribution of small spheres ('ballotini') stuck onto the wing surface in a thin band at about 5% chord back from the leading edge. At the Reynolds numbers of the tests the diameter of the spheres was very small compared with the wing chord, a diameter-to-chord ratio of 0.00015 being typical. This approach avoided the location of the transition region having to be determined for each combination of free-stream Mach number and wing incidence, and it also ensured transition would occur near the leading-edge of the wings at an almost constant location on the chord, thus helping to ensure two-dimensional flow.

Although there is some uncertainty about the transition process itself, it is thought that in terms of the chord the boundary-layer flow settles down to a truly turbulent layer quite quickly[3] after transition has occurred.

Wind Tunnel Wall Corrections

Wind tunnel wall effects manifest themselves in several ways. The pressure distribution on the wing can be influenced as a direct result of the pressure field generated by the presence of the walls, but in addition the boundary-layer growth on both the wind tunnel walls and the wing can be altered. Thus the pressure distribution on the wing itself is altered. As far as the boundary-layer growth on the wing is concerned, the changes due to flow convergence generated at the ends of a wing can be significant but an allowance may be made for this as pointed out by Bradshaw[4]. The span:chord ratios of the wings of these tests were quite large (3:1) so any corrections on this account should be small. In addition sufficient information has been obtained, provided the skin friction measurements are reliable, to determine the influence of the convergence term in the boundary-layer equations and hence an estimate of this can be made if necessary.

As far as the direct pressure interference from the constraints of the tunnel walls are concerned, these are usually assumed to be calculable[5] in solid-wall tunnels, but when the walls are slotted the methods are very doubtful due to the influence of viscosity on the slot effectiveness. It is thus essential to find a method such that the corrections may be determined experimentally. One method we have tried is to test two symmetrical wings of the same cross-section but with different chords at the same Reynolds number and with transition bands of the same size relative to the chord[6]. The open-area ratio of the tunnel walls was chosen so that the influence of the excess velocity due to blockage was negligible over a range of Mach numbers, this was done by comparing the pressure distributions on the two wings at zero incidence. Measurements were then made for the two wings over a range of incidence and Mach number, and it was assumed that the interference occurred as an upwash at the centre of pressure with a rate of change in upwash along the chord. If we then follow a standard method of calculating wind tunnel wall interference effects we may write[5]

$$\frac{\Delta\alpha}{C_L} = \left[\frac{c}{h}\right]\psi_o + \left[\frac{c^2}{\beta h^2}\left(\frac{1}{4} + \frac{C_m}{C_L}\right)\right]\psi_1$$

$$\frac{\Delta C_L}{C_L} = \left[-\frac{\pi}{2}\left(\frac{c}{\beta h}\right)^2\right]\psi_1$$

$$\frac{\Delta C_m}{C_L} = \left[\frac{\pi}{8}\left(\frac{c}{\beta h}\right)^2\right]\psi_1$$

where C_L and C_m are the measured values.
The coefficients ψ_o and ψ_1 can be obtained experimentally and thus the interference terms are determined completely. This method of analysis allows for any form of interference which is dependent linearly upon C_L and which may be represented by an upwash and a rate of change in upwash along the chord. This does not exclude interference from the loss of lift at the ends of the wings or from any object in the wind tunnel, provided the tunnel height is redefined as the tunnel scale, but it implies that the flow is not truly two-dimensional and the angle of incidence would therefore, be a function of spanwise location.

Returning now to the detailed analysis, it was found that the variation of lift and pitching-moment coefficient against angle of incidence could not be represented adequately by a linear form over the range ±4 degrees, so it was assumed that $C_L = a_1\alpha + b_1\alpha^3$ and $C_m = a_2\alpha + b_2\alpha^3$. In addition, the rather more dubious assumption was made that b_1 and b_2 were unaltered by wind tunnel interference. ψ_o and ψ_1 were then determined from the derived slope near zero incidence, $\left(\frac{\partial C_m}{\partial C_L}\right)_{\alpha=0}$ for the two wings being sufficient to determine ψ_1 and $\left(\frac{\partial C_L}{\partial \alpha}\right)_{\alpha=0}$ being used to find ψ_o. This method of analysis made some assumptions about the form of interference but these may be checked by comparing the corrected measurements for the two wings. Figure 4 gives the results of such an analysis at two Mach numbers for both the slotted-wall tunnel and for the same tunnel with all the slots sealed. This figure shows the deduced variation of the lift curve slope with tunnel size, and the experimentally determined lift-curve slopes, which are corrected for the effects of wind tunnel blockage, are also given. As the deduced variation of lift curve slope

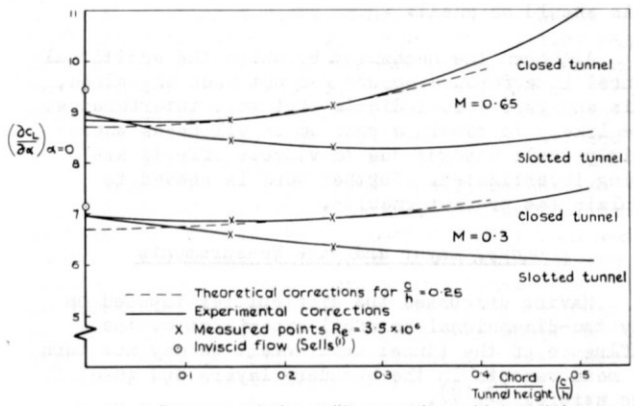

Fig. 4 Deduced variation of lift curve slope with tunnel size for RAE 101 section with 10% thickness: chord ratio·

with tunnel size is non-linear it is clear for both wind-tunnel configurations, that the walls induce a curved flow over the wing and consequently any corrections made can only be considered to be accurate within the limitations of a first-order theory. For the slotted-wall tunnel configuration, it should be possible to find an open-area ratio for the walls at which the induced flow is not curved, but this can only be done at the expense of an uncertainty in the blockage corrections especially at high subsonic speeds. Returning now to Figure 4, the interference free results are obtained from the values at which the ratio of chord to tunnel height is zero. The interference coefficients for the slotted-wall tunnel are broadly in agreement with the trends suggested by the theory. On the other hand the deduced lift curve slopes are

larger than had been anticipated and this suggests that the boundary-layers and the wake of the wings have a smaller influence than had been expected. Results for the closed-wall tunnel for which theoretical blockage corrections have been applied confirm the findings for the slotted-wall tunnel but are not in very good agreement with the expected theoretical corrections which are given for the larger wing by the dashed curve in the figure. The theoretically corrected lift curve slop is 4% below the experimentally deduced value at a stream Mach number of 0.3 and 2% at a Mach number of 0.65. A 3% difference in lift curve slope would account for about 13% of the difference between the measured pressure distribution and the inviscid flow calculation given in Figure 1. This shows that there is some uncertainty in the tunnel corrections; it is not clear why the closed-wall tunnel results give a slightly higher lift curve slope than that suggested by the theoretical corrections but one possible reason is that a loss of lift is occurring at the intersection between the wings and the tunnel walls due to an interaction between the boundary layers. Preston[7] has given a rather simplified method for calculating this effect, for incompressible flows, where he allows the sectional lift to fall unrealistically to zero at the tunnel wall, but this would account for only 0.5% of the loss of lift at the centre-line of the wind tunnel. The measurements of Mendelsohn and Polhamus[8] shows that in practice the loss of lift at the tunnel walls is only about 10%, resulting in a much smaller downwash at the centre of the tunnel than given by Preston. Another possible cause of the measured downwash is interference from the traverse support rig which is well downstream of the wing, but here again simplified calculations suggest that the interference from this should be small.

Although the mechanism by which the additional tunnel interference occurs has not been explained, this analysis does indicate that wall interferences are likely to remain a problem in all cases where fairly small changes due to viscous effects are being investigated. Further work is needed to explain the present results.

Boundary Layer and Wake Measurements

Having discussed the difficulties imposed on any two-dimensional aerofoil experiment by the influence of the tunnel environment we may now turn to measurements in the boundary layers and wake of the aerofoil[9,10].

We are interested here in the mean flow over an aerofoil since this will be responsible for the steady forces, and although the turbulent structure of the boundary-layer may be important in formulating adequate prediction methods for boundary-layer and wake growth, we have not attempted to make any such measurements. To determine the mean boundary layer or wake characteristics in compressible flow, we strictly require measurements of the mean temperature distribution in addition to pitot and static pressure measurements, but at subsonic speeds the influence of various plausible assumptions about the variation in the total temperature through the boundary layer makes only a very small difference to the velocity distribution and consequently no attempt was made to obtain such measurements[11].

It is usually assumed that the static pressure variation through the layer may be neglected, but near the trailing edge of an aerofoil where the flow is highly curved this is not acceptable and some measurements have been made therefore with a static probe. It was found that at all stations other than those within a few per cent chord of the trailing-edge of the wing, the variation of static pressure was negligible and consequently the measured surface pressure has been used as the local static pressure and in the wake a mean value has been taken from a wake traverse for most of the analysis.

Figure 5 shows the growth of the boundary-layer and wake in a typical case. This is for a symmetrical RAE 101 section with a lift coefficient of about 0.5. The boundary layer grows about twice as fast on the upper surface as on the lower surface, and by the time the trailing-edge is reached, its total thickness is nearly half the maximum aerofoil thickness. Downstream of the trailing-edge the minimum velocity increases rapidly from zero while the profiles deform in the region of maximum shear until the wake becomes almost symmetrical. These results are similar of course, to those found by others such as Preston et al[12,13] on wing sections at low speed and lower Reynolds numbers.

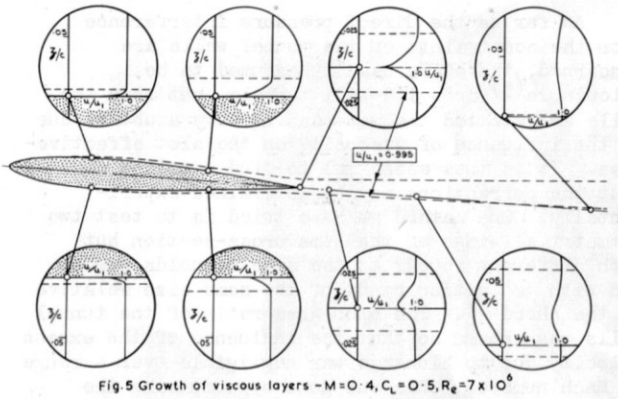

Fig.5 Growth of viscous layers - $M=0.4, C_L=0.5, R_e=7\times10^6$

The boundary-layer integral parameters, the displacement and momentum thicknesses, are also of interest. By definition, the displacement thickness is the distance by which the surface streamlines must be displaced in order that the influence of the boundary layer on the external streamline flow may be simulated, and the momentum thickness gives a measure of the loss of momentum due to the presence of the boundary layer and therefore gives a measure of the drag. In Figure 6, measurements of the displacement thickness are given for three different conditions covering a range of speeds and pressure distributions. One condition shown is for a symmetrical RAE 101 section at zero incidence near the critical speed, while another is at a lower speed but at an angle of incidence which results in an adverse pressure gradient on the upper surface from a point near the nose to the trailing-edge. The third gives perhaps a more severe test since this is for a cambered wing with a 'sonic' roof-top pressure distribution back to 35% chord combined with higher adverse pressure gradients on both upper and lower surfaces. In all these three cases the boundary-layer grows most rapidly over the rear of the wings where the adverse pressure gradients are largest.

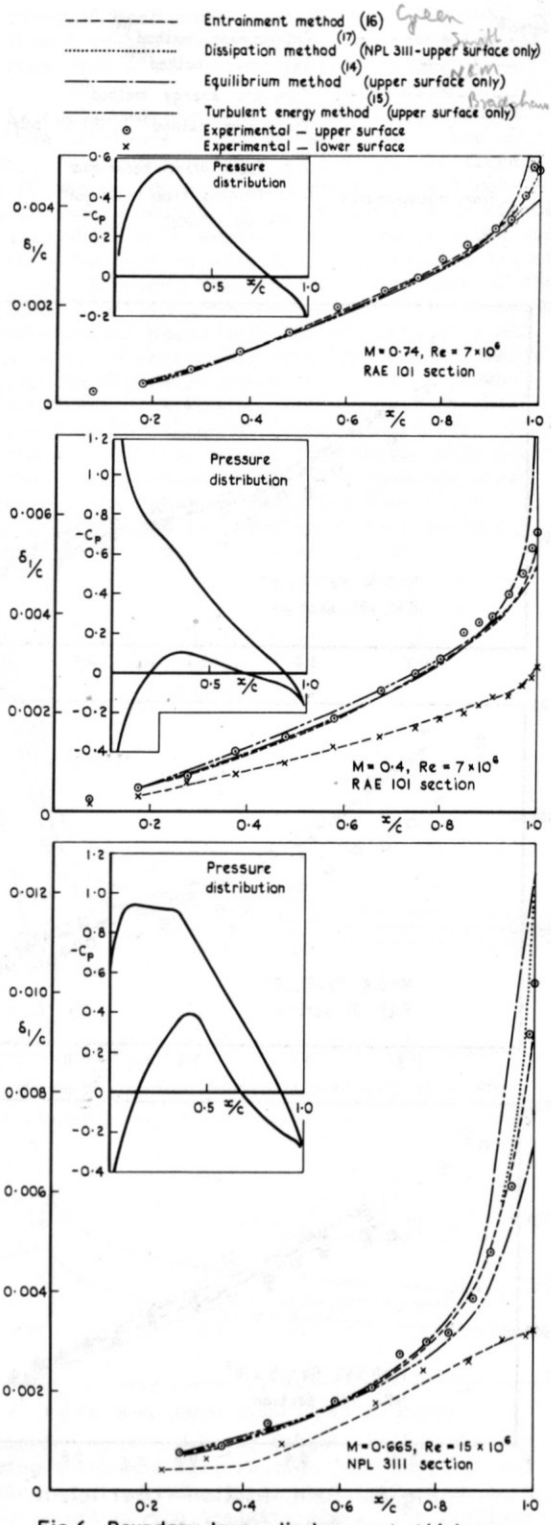

Fig.6 Boundary layer displacement thickness

A selection of boundary-layer prediction methods have been tried[14,15,16,17], without any allowance for spanwise convergence. They tend to predict the same growth as the measurements show over the central part of the chord where the rate of growth is moderate, but over the rear of the wings where the rate of growth is larger as a result of the larger adverse pressure gradients, the methods disagree. It appears that as far as displacement effects are concerned the equilibrium method[14] tends to over-estimate the influence of the pressure gradient near the trailing-edge of the wings, and the turbulent energy method[15] underestimates this. From these comparisons it is not clear whether the presence of the trailing-edge of a wing has a significant influence on the manner by which the boundary-layer grows. The differences between the theories which are apparent over the rear of the aerofoils would make any attempt to estimate form-drag accurately very difficult.

The momentum thickness for the same three conditions is given in Figure 7 and comparisons with the same theories are also given. Once again the trends are well predicted by the theories but there are differences of about 20% at the trailing-edge of the wings. This kind of difference is of course very important as it is directly related to errors in profile-drag estimation. We will return to this later when drag measurements are discussed.

Another important measurement that has been made on the aerofoil surface is the skin friction. If this can be measured accurately enough, as mentioned before, we have sufficient information to study all the terms in the momentum integral equation and the influence of spanwise convergence. Spanwise convergence should not be a serious problem in these tests since the measurements were made on wings of high aspect-ratio, and in addition some checks using surface oil studies over the outboard regions of one of the wings (RAE 101 section) showed that there was no significant divergence from two-dimensional flow in those regions.

Skin friction could not be measured directly but was determined by the 'razor-blade' method. This technique consists of forming a surface pitot tube by sticking a small segment of razor blade onto the wing surface with its tapered cutting edge directly above a static pressure hole. The method has been explored by Smith, Gaudet and Winter[18] for compressible flows, and it was a 'flat-plate' calibration derived from their work that was used for our measurements. Figure 8 gives the measurements made for the same three conditions that we considered before. The skin friction coefficient is based on the flow in the undisturbed stream and consequently gives a direct representation of the change in shear stress along the surface. The measurements, particularly for the low speed case on the RAE 101 section, are lower than would be expected and the reason for this is not yet understood. A systematic study of the use of razor blades for skin friction measurements by East[19] at low speeds does not indicate any cause for this discrepancy, and the use of his calibration gave almost the same results. The measurements were, of course, made on a curved surface in a pressure gradient and it is not known how measurements by this technique are affected by these factors. The evidence obtained so far however, indicates that the difference between theory and measurement are independent of pressure gradient and the local surface curvature. A further check was possible for the measurements on the NPL 3111 section using the Preston tube technique, with a calibration due to Hopkin and Keener[20] for compressible flow; these measurements are broadly in agreement with the 'razor blade' method. It was also possible to deduce the skin friction from the measurements of the boundary layer profiles near the wing surface by assuming a 'law of the wall' holds. The results

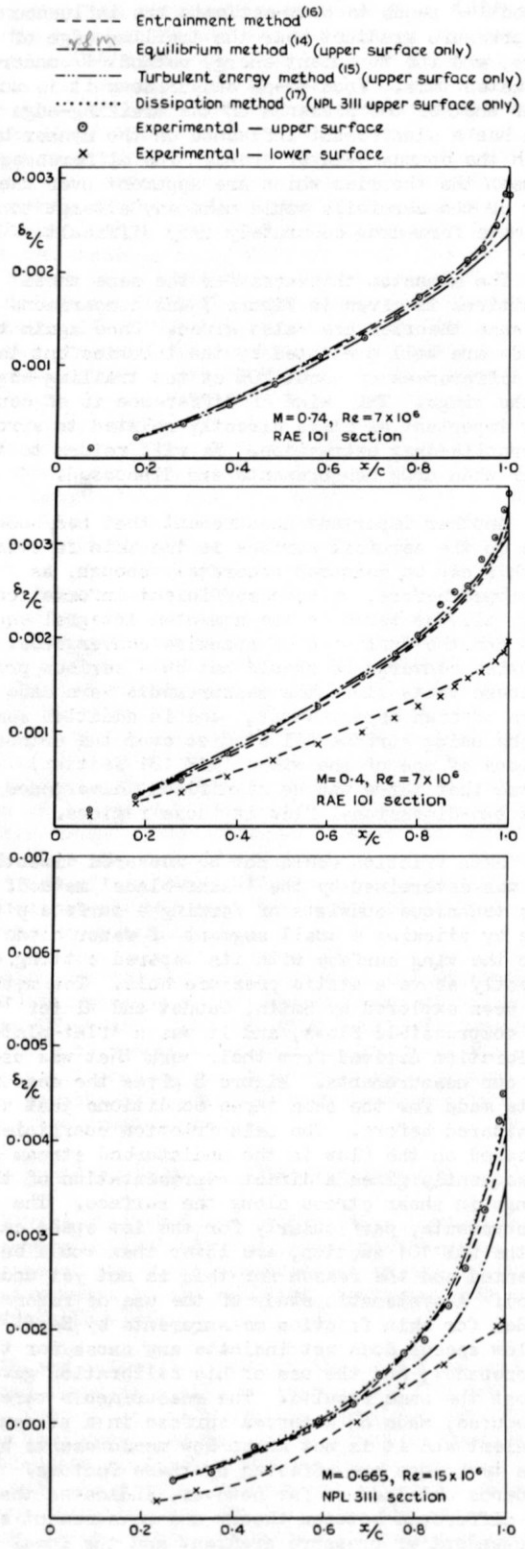

Fig.7 Boundary layer momentum thickness

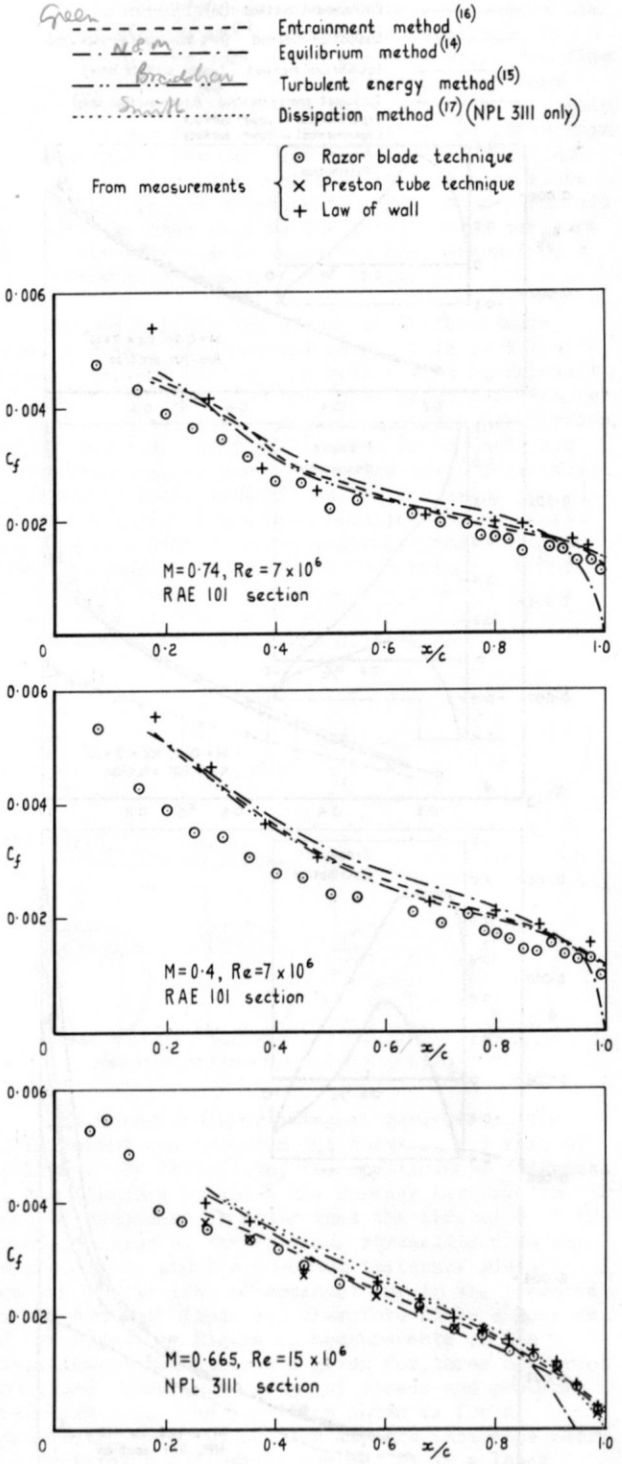

Fig. 8 Skin friction coefficient (upper surfaces)

deduced were obtained from the 'law of the wall' given by Winter and Gaudet[21], but similar results would have been obtained using the values for the constants given by Coles[3]. This analysis usually gives higher values for the surface friction than those obtained by the surface tube techniques. This is particularly true at the lower Mach numbers and the authors thus have doubts on these surface tube methods of determining skin friction and the constants generally assumed in the law of the wall. Further work is required to determine the causes of the discrepancies found. The existing boundary-layer methods which use various skin friction laws tend to support in general the 'law of the wall' results.

Other aspects of the work on boundary layers such as a detailed study of the changes in the velocity profiles in the presence of pressure gradients will be studied later. Measurements have so far been made for about twelve different

conditions of Mach number and lift-coefficient, this should enable a systematic analysis to be performed over a wide range of conditions.

As mentioned previously there is some doubt about the influence of the curved flow in the region of the trailing edge of a wing. In these tests it was not possible to measure flow directions in such a region due to the small size of the region in which such measurements were required and this is to be done separately on a special model at low-speed. Measurements, however, were made of the variation of static pressure and the displacement and momentum thickness near the trailing-edge and in the wake. Some results from these measurements are given in Figure 9a where the total displacement thickness of a wing is plotted against chordwise position for three different conditions. The displacement surfaces appear to be reasonably smooth near the trailing-edge of the wing when the wing thickness is included as well, but there is a fairly rapid change in the displacement surface slope in the region of the trailing-edge.

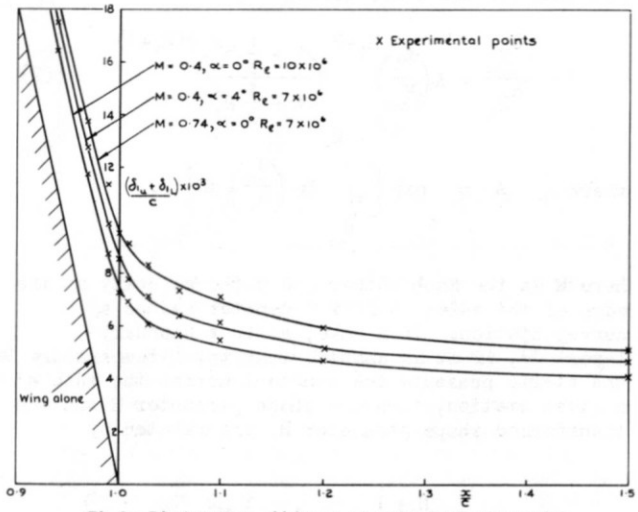

Fig.9a Displacement thickness of wake-RAE 101 section

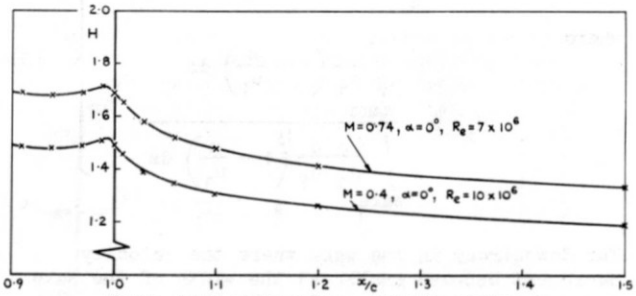

Fig.9b Wake shape factor – RAE 101 section

The displacement thickness follows fairly closely the wing thickness distribution just ahead of the trailing-edge and then turns rapidly for the next 10% chord aft of the trailing-edge. The displacement thickness then contracts slowly over the region up to two chords behind the wing, the furthest point behind the wing at which measurements were made. In Figure 9b the shape factor in the wake is given for the wing at zero incidence ($C_L = 0$). It should be noted, however, that the shape factor does not drop to unity. In these tests, at a Mach number of 0.74 and an incidence of zero, the wake shape factor was still 1.3 two chords behind the wing and the displacement thickness was therefore closely approximated by

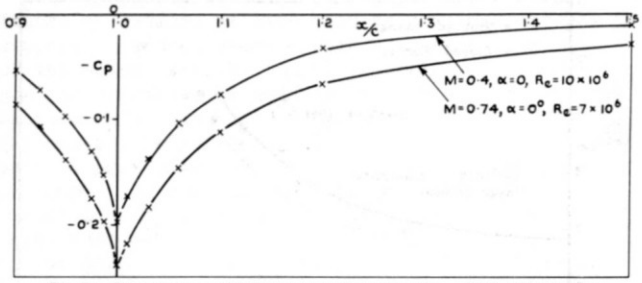

Fig. 9c Pressure coefficient at centre of wake - RAE 101 section

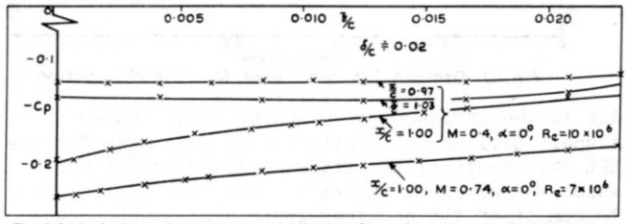

Fig.9d Variation of pressure coefficient through wake - RAE 101 section

$1.3 \times C_D/2$ and not $C_D/2$ as generally assumed. The next part of the figure (Figure 9c) shows the variation of static pressure in the region of the trailing-edge. These results, which are for the pressure at the centre of the wake, are consistent with the variation expected from the displacement surface, the highest pressure occurring where the curvature is greatest. When considering whether the flow in the trailing-edge region may be considered as a boundary-layer, a difficulty occurs due to the variation in static pressure through the layer. Measurements of this are shown for three chordwise locations in Figure 9d. It is clear that for this simple case of a wing at zero incidence, the static pressure may be considered constant for all stations other than those within a few per cent chord of the trailing-edge. Curvature of the flow in the sense found near the trailing-edge would be expected to lead to a change in pressure as observed.

Overall Forces

Lift

From the evidence available it is difficult to assess the influence of the various effects on lift due to uncertainties in the wind tunnel wall corrections. Generally speaking previous evidence has suggested that for a wing section with pressure distributions of the form we have shown, the loss in lift at the quoted Reynolds numbers would be about 10% for the RAE 101 section, and perhaps 20% for the other wing with a larger rear loading. The recent work on tunnel corrections indicates that at least part of this could be accounted for by tunnel corrections. For the RAE 101 section the uncertainty in wind tunnel wall corrections represents a change between 2% and 4% in the lift curve slope. Figure 10 gives a comparison between the measured lift curve slopes and the values from exact inviscid theory[1]. The measured values of lift curve slope are within 5% of the theoretical values over the range where calculations have been made, and this is rather less than that found previously at low speeds[22]. An estimate for the loss in lift expected due to the camber of the boundary-layer displacement surface has been obtained from linearised theory and is also given in the figure. This suggests that about a 6% loss in lift occurs

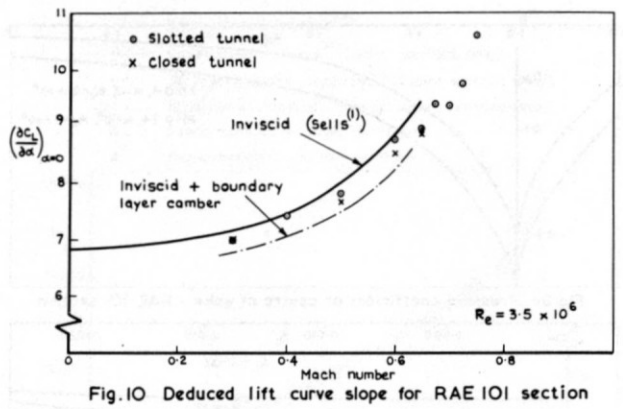

Fig.10 Deduced lift curve slope for RAE 101 section

due to the influence of boundary layer camber alone. Similar calculations have been made for the NPL 3111 section, the pressure distribution for which was given in Figure 1. The loss in lift due to camber of the boundary-layer displacement surface was 0.145, suggesting a lift coefficient of 0.520 compared with the measured value of 0.515. Applying theoretical wind tunnel wall corrections to the measured value gave a lift coefficient of 0.485 leaving the measurements about 7% below the calculation corrected for the influence of boundary layer camber. Some of this difference may be accounted for by uncertainty in wind-tunnel wall corrections, but we are left with a situation where for two aerofoil sections, which have very different chordwise loadings, the remaining inadequacies in possible theoretical treatments, such as the Kutta condition at the trailing edge and the influence of a curved wake, must give a contribution to the lift of opposite sign. This problem may be resolved as the measurements are analysed further.

Drag

Turning now to the important subject of drag we consider first the determination of drag by wake or trailing-edge boundary-layer surveys. These are used to calculate the effective momentum thickness of the wake far downstream of the wing and thence drag by an application of the momentum theorem.

The expression for drag in terms of the far downstream momentum thickness δ_{2_∞} is usually given as

$$C_D = 2 \cdot \frac{\delta_{2_\infty}}{c}$$

(this follows from Ref.23 for example). In a wind tunnel which is not interference-free this expression requires a little modification since the velocity outside the wake far downstream differs from the velocity far upstream of the model as a result of wake blockage, and both these velocities differ from the effective free-stream velocity at the position of the model because of solid and wake blockage. The momentum theorem then gives drag by

$$C_D = \left\{ C_{p_e} H_\infty + 2 \right\} \frac{\delta_{2_\infty}}{c} \cdot \frac{q_\infty}{q_{ref}} \quad . \qquad (1)$$

Here H_∞ is the shape parameter, δ_1/δ_2, and q_∞ is the kinetic pressure of the wake far downstream. q_{ref} is the kinetic pressure used as reference pressure in evaluating C_D, C_{p_e} is a pressure coefficient $(p_e - p_\infty)/q_\infty$, where p_∞ is the static pressure outside the wake far downstream and p_e is the static pressure far upstream of the model. C_{p_e} is assumed to be small.

In a tunnel which has a pressure gradient along it when empty, an effective upstream static pressure p_e can be defined as the static pressure in the empty tunnel at the wake survey station. However the effect of tunnel interference on measurements of drag obtained by wake surveys needs further clarification. Some work on this topic has been done by Ritter[24].

The wake momentum thickness far downstream of the wing may be calculated in terms of upstream measurements by integration of the momentum integral equation for the wake, giving

$$\frac{\delta_{2_\infty}}{\delta_{2_1}} = A \left(\frac{M_1}{M_\infty}\right)^{H_1+2} \left(\frac{1 + \frac{1}{5} M_\infty^2}{1 + \frac{1}{5} M_1^2}\right)^{\frac{1}{2}(H_1+7)} \qquad (2)$$

where $$A = \exp\left\{ \int_{H_\infty}^{H_1} \ln\left(\frac{u_\infty}{u_1}\right) dH \right\} .$$

Here M is the Mach number and u the velocity at the edge of the wake; suffix 1 denotes values at a survey station. In a wake, as in a boundary-layer[25], if it is assumed that total temperature and static pressure are constant across the wake at a given station, then the shape parameter H and the transformed shape parameter H_i are related by

$$\left.\begin{aligned} \frac{H + 1}{H_i + 1} &= 1 + \frac{1}{5} M^2 \quad , \\ \text{where} \qquad H_i &= \frac{\int_{\text{wake}} \frac{\rho}{\rho_1}\left(1 - \frac{u}{u_1}\right) dz}{\int_{\text{wake}} \frac{\rho\, u}{\rho_1\, u_1}\left(1 - \frac{u}{u_1}\right) dz} \quad . \end{aligned}\right\} \qquad (3)$$

Far downstream in the wake where the velocity decrement becomes small and the width of the wake large H_i tends to unity and H_∞ becomes $1 + \frac{2}{5} M_\infty^2$. This value is used here. The evaluation of the exponential factor in equation (2) was considered by Squire and Young[26] who decided on a linear relationship between $\ln\left(\frac{u_\infty}{u_1}\right)$ and H downstream of the wing trailing-edge. If we make this assumption here equation (2) is simplified to

$$\frac{\delta_{2_\infty}}{\delta_{2_1}} = \left(\frac{M_1}{M_\infty}\right)^{\frac{1}{2}(H_1+H_\infty+4)} \left(\frac{1 + \frac{1}{5} M_\infty^2}{1 + \frac{1}{5} M_1^2}\right)^{\frac{1}{4}(H_1+H_\infty+14)} \quad . \qquad (4)$$

We have found the Squire and Young assumption to be a reasonable approximation for the shape factor in the wake of wings when the shape factor at the trailing-edge is not too large, i.e. the boundary-layer on either surface is not near separation. Figure 11, however, shows what happens in the case of a section when the trailing-edge boundary-layer on the upper surface has been considerably thickened by the severe adverse pressure gradient following a 55% chord 'sonic rooftop'. Here the variation of H with $\ln(u_\infty/u_1)$ is far from linear; nevertheless, as the insert table shows, the loss

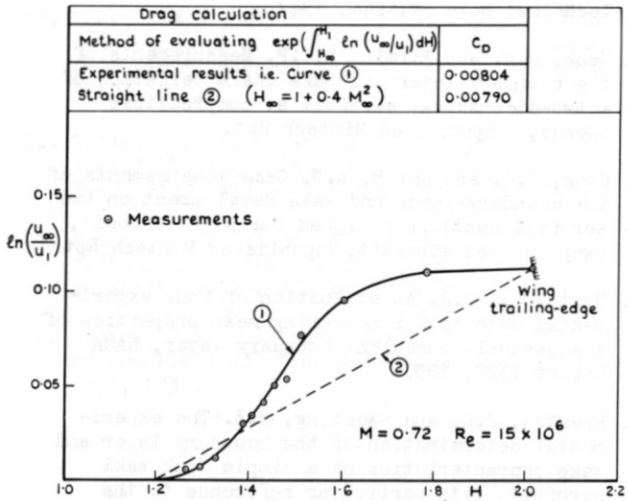

Fig 11 Variation of H with $\ln(u_\infty/u_1)$ in wake and deduced values of profile drag

of accuracy in making the Squire and Young assumption from the trailing-edge is not large. For surveys made progressively further downstream, errors due to making the Squire and Young assumption will decrease and for the results shown they are negligible for surveys made more than about 10% aft of the trailing-edge. Equation (4) should then be very accurate.

Figure 12 shows the drag results obtained from surveys made at various chordwise stations downstream of the trailing-edge by the method described above, and the effect of chordwise station is, in

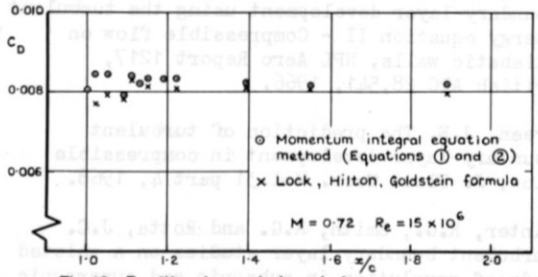

Fig.12 Profile drag deduced from measurements at various wake stations

fact, seen to be small. All the results are within the range $C_D = 0.0082 \pm 0.0003$. Also shown are the results of calculations made by the method of Lock, Hilton and Goldstein[23]. This method includes the assumption that total pressure is constant along streamlines in the wake, downstream of the measuring station. These results are seen to be about 0.0002 low for surveys aft of about 10% chord from the trailing edge.

In the work in the 8 ft x 8 ft (2.4 m x 2.4 m) tunnel at Bedford we have been able to make three-component balance measurements on part of the span of the model near the tunnel centreline. A comparison can therefore be made between three sets of drag measurements, viz. (1) wake survey results, (2) balance measurements, and (3), integration of surface pressures and shear stresses. Balance and pressure measurements are fully corrected for tunnel interference effects and pressure measurements must be corrected for errors due to the finite diameter of each orifice. Such a comparison is made in Figure 13, where the full line is the mean of a comprehensive set of balance measurements.

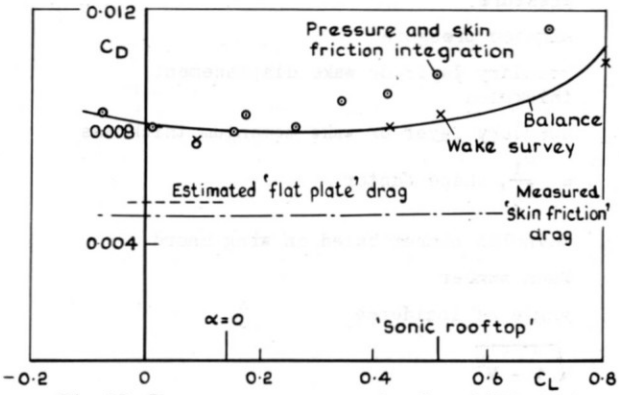

Fig.13 Drag measurements for NPL 3111 section at M = 0·665, R = 15·6 x 10⁶

It must be pointed out however, that accurate balance results were only obtained by leaving a small, unsealed gap of width 0.02% chord at the edges of the 'live' panel. The effect of this gap on drag is thought to be small and this is confirmed to some extent by the fair agreement shown between the balance and wake survey results. There is a tendency in this and other work, however, for wake survey measurements to give drags a little below corresponding balance measurements. Integration of surface pressures and skin friction is the least precise of all the methods, and this is to some extent demonstrated by the scatter of the results. The results show good agreement with other methods at low lift but a considerably greater increase in drag with increasing lift. At the moment the reasons for this discrepancy are not fully understood.

Also included in Figure 13 are skin friction drag measurements. These are typical of the results obtained for this component, drag being rather less than the corresponding flat plate estimate and insensitive to lift.

Conclusions

We have highlighted some of the difficulties encountered in making measurements on two-dimensional aerofoils and have indicated some of the problems which the results should help to resolve. The analysis of the experimental evidence obtained, however, is not complete and certain features of the work need further checking. We set out to provide a definitive set of measurements to help consolidate the methods of prediction for loads on two-dimensional aerofoils at compressible speeds, and this much, we hope, we have achieved.

Symbols

C_D	profile drag coefficient
C_f	skin friction coefficient (based on undisturbed stream)
C_L	lift coefficient
C_m	pitching moment coefficient
C_p	pressure coefficient
c	chord
h	wind-tunnel height
p	pressure
q	kinetic pressure
δ_1	boundary layer or wake displacement thickness
δ_2	boundary layer or wake momentum thickness
H	$= \frac{\delta_1}{\delta_2}$, shape factor
Re	Reynolds number based on wing chord
M	Mach number
α	angle of incidence
β	$\sqrt{1 - M^2}$
ψ_o, ψ_1	coefficients for wind tunnel wall corrections
U	velocity
x	chordwise location measured from leading edge of wing
z	distance from surface or chordline

Suffices

∞	far downstream
e	far upstream
1	local value outside boundary-layer or wake
u	upper surface
ℓ	lower surface

References

1. Sells, C.C.L. Plane subcritical flow past a lifting aerofoil, RAE TR 67146, 1967.

2. Küchemann, D. Inviscid shear flow near the trailing edge of an aerofoil, RAE TR 67068, 1967.

3. Coles, D.E. The turbulent boundary layer in a compressible fluid, The Rand Corporation R-403-PR, 1962.

4. Bradshaw, P. and Ferriss, D.H. The response of a retarded equilibrium turbulent boundary layer to the sudden removal of pressure gradient, NPL Aero Report 1145, British ARC 26758, 1965

5. Garner, H.C., Rogers, E.W.E., Acum, W.E.A. and Maskell, E.C. Subsonic wind tunnel wall corrections, AGARDograph 109, 1966.

6. Bartlett, R.S. and Firmin, M.C.P. Experimental determination of subsonic wind tunnel wall corrections, Unpublished Mintech Rpt.

7. Preston, J.H. The interference on a wing spanning a closed tunnel, arising from the boundary layer on the side walls, with special reference to the design of two dimensional tunnels, British ARC R& M 1924, 1944.

8. Mendelsohn, R.A. and Polhamus, J.F. Effect of the tunnel-wall boundary layer on test results of a wing protruding from a tunnel wall, NACA Technical Note No.1244, 1947.

9. Cook, P.H. and Firmin, M.C.P. Measurements of the boundary layer and wake characteristics of a two-dimensional aerofoil at compressible speeds, Unpublished Mintech Rpt.

10. Cook, T.A. and Smith, A.W. Some measurements of the boundary-layer and wake development on two aerofoil sections designed for high subsonic, swept winged aircraft, Unpublished Mintech Rpt.

11. Northwong, G.J. An evaluation of four experimental methods for measuring mean properties of a supersonic turbulent boundary layer, NACA Report 1320, 1957.

12. Preston, J.H. and Sweeting, N.E. The experimental determination of the boundary layer and wake characteristics of a simple Joukowski aerofoil, with particular reference to the trailing edge region, British ARC R& M 1998, 1943.

13. Preston, J.H., Sweeting, N.E. and Cox, D.K. The experimental determination of the boundary layers and wake characteristics of a Piercy 12/40 aerofoil, with particular reference to the trailing edge region, British ARC R& M 2013, 1945.

14. Nash, J.F. and Macdonald A.G.T. The calculation of momentum thickness in a turbulent boundary layer at Mach numbers up to unity. NPL Aero Report 1270, British ARC 28,235, 1966.

15. Bradshaw, P. and Ferriss, D.H. Calculation of boundary-layer development using the turbulent energy equation II - Compressible flow on adiabatic walls, NPL Aero Report 1217, British ARC 28,541, 1966.

16. Green, J.E. The prediction of turbulent boundary-layer development in compressible flow, J. Fluid Mech. Vol.31 part 4, 1968.

17. Winter, K.G., Smith, K.G. and Rotta, J.C. Turbulent boundary layer studies on a waisted body of revolution in subsonic and supersonic flow, AGARDograph 97 (Part 2) pp. 933-962, 1965.

18. Smith, K.G., Gaudet, L. and Winter, K.G. The use of surface pitot tubes as skin friction meter at supersonic speeds, British ARC R& M 3351, 1962

19. East, L.F. Measurement of skin friction at low subsonic speeds by the razor-blade technique. RAE TR 66277, 1966.

20. Hopkins, E.J. and Keener, E.R. Study of surface pitots for measuring turbulent skin friction at supersonic Mach numbers - adiabatic wall. NASA TN D 3478, 1966.

21. Gaudet, L. and Winter, K.G. Turbulent boundary-layer studies at high Reynolds numbers, at Mach numbers between 0.2 and 2.8, Unpublished Mintech Rpt.

22. Brebner, G.G. and Bagley, J.A. Pressure and boundary layer measurements on a two-dimensional wing at low speed, British ARC R& M 2886, 1956.

23. Lock, C.W.H., Hilton, W.F. and Goldstein, S. Determination of profile drag at high speeds by a pitot traverse method, British ARC R& M 1917, 1940.

24. Ritter, H. Wake traverse in the presence of tunnel blockage, Admiralty Research Lab. Teddington, Middx, England, ARL/G/NA, 1963.

25. Spence, D.A. The growth of compressible turbulent boundary layers on isothermal and adiabatic walls, RAE Report Aero 2619, 1959.

26. Squire, H.B. and Young, A.D. The calculation of profile drag of aerofoils, British ARC R& M 1838, 1937.